1995

Theoretically Optimal Duty Cycles for Chest and Abdominal Compression during External Cardiopulmonary Resuscitation

Charles F. Babbs
Purdue University, babbs@purdue.edu

Keir Thelander

Theoretically Optimal Duty Cycles for Chest and Abdominal Compression during External Cardiopulmonary Resuscitation

Charles F. Babbs, MD, PhD, Keir Thelander, BS

Biomedical Engineering Center, Purdue University, West Lafayette, Indiana, USA.

ABSTRACT

Objective: To use an electronic model of human circulation to compare the hemodynamic effects of different durations of chest compression during external CPR, both with, and without interposed abdominal compression (IAC).

Methods: An electrical analog model of human circulation was studied on digital computer workstations using SPICE, a general-purpose circuit simulation program. In the model the heart and blood vessels were represented as resistive-capacitive networks, pressures as voltages, blood flow as electric current, blood inertia as inductance, and cardiac and venous valves as diodes. External pressurization of the heart and great vessels, as would occur in IAC-CPR, was simulated by the alternate application of damped rectangular voltage pulses, first between intrathoracic vascular capacitances and ground, and then between intra-abdominal vascular capacitances and ground. With this model, compression frequencies of 60, 80, and 100 cycles/min and duty cycles ranging from 10% to 90%, both with and without IAC, were compared.

Results: There was little difference in hemodynamics when the overall compression frequency was varied between 60 and 100 cycles/min; but the effects of duty cycle were substantial. During both standard CPR and IAC-CPR, total flow and coronary flow were greatest at chest compression durations equal to 30% of cycle time. Interposed abdominal compression substantially improved simulated systemic blood flow and perfusion pressure at all duty cycles, compared with standard CPR without abdominal compression. Mean arterial pressure > 75 mm Hg and artificial cardiac output > 2.0 L/min could be generated by 30% duty cycle compression with IAC. Coronary perfusion in the model is clearly optimized at 30% chest compression (i.e., high-impulse chest compression technique).

Conclusion: Combined high-impulse chest compressions and IACs maximize blood flow during CPR in the electrical analog model of human circulation.

Key words: abdominal; artificial circulation; blood flow; cardiac arrest; CPR; high impulse compression, HIC, interposed abdominal compression, IAC

INTRODUCTION

Timing variables describe, in a fundamental way, how external CPR is done. The most obvious timing variables are the compression rate or frequency, or its inverse, the total cycle time. Other key timing variables describe the partitioning of the CPR cycle time into chest compression and chest relaxation phases. During ordinary standard CPR, the duty cycle of compression refers to the fraction of cycle time during which active chest compression is applied. The issue of the most effective compression frequency and duty cycle in standard external CPR is of considerable importance, owing to research over the past decade by Maier et al. [1, 2], Swart et al. [3], and Swenson et al. [4] suggesting that shorter chest compression times comprising 30% of the total compression cycle, which they characterize as "high velocity, moderate-force, and brief-duration manual compressions," are more effective in producing forward flow than what has come to be accepted as the standard, 50% duty cycle for chest compression.

The optimization of timing variables in external CPR is further complicated by the addition of interposed abdominal compressions (IACs), which have proved to constitute a promising adjunct to conventional CPR [5]. This manual technique can supplement the use of adrenergic drugs to increase coronary perfusion pressure (CPP) and total blood flow during resuscitation [6-10]. Clinical studies confirm that IAC-CPR can improve perfusion pressures and CO_2 excretion during CPR in humans [11-13], and a randomized trial has shown that short-term and long-term survival rates for patients resuscitated in the hospital with IAC-CPR can be twice those for control patients resuscitated by standard CPR [5, 14]. However, the exact technique by which abdominal compressions are best applied is controversial [15-18]. Differences in the site, area, angle, and force of IACs have been discussed elsewhere [15, 17]. With two notable exceptions [19, 20], the timing variables of IAC-CPR have been largely neglected, and the combination of high-impulse compression (HIC) with IAC-CPR has not been explored.

To study the complex effects of varying chest and abdominal compression times, we turned to a computer model that has proved insightful in the past for understanding and predicting the hemodynamics of resuscitation and of cardiac assist devices [21-23]. Because such models are much simpler than intact animals and allow easy manipulation of system parameters, it is possible to evaluate a large number of timing variables and to understand their contribution to simulated flow. Our study was conducted to address the theoretically optimal duty cycle for chest compression during standard CPR and also to assess the theoretically optimal temporal partitioning of external compression between chest and abdominal phases during interposed abdominal compression CPR.

METHODS

Study Design

We investigated CPR duty cycle variables using a simple resistive-inductive-capacitive model of circulation, in which flow can be generated by simulated external compression of the heart, the intrathoracic great vessels, the abdominal aorta, or the abdominal veins (by applying voltage

pulses to particular sets of capacitors), and in which phased chest and abdominal compressions of varying duty cycles can be simulated.

Model of the Circulatory System

Our electrical analog model of human circulation is shown in Figure 1. In the model the great vessels and cardiac chambers are modeled as capacitors, and capillary beds are modeled as resistors. The flow of electric current around the circuit (arrows) represents the flow of blood, and the action of the arterial and venous inductors models the inertia of the blood columns in the larger, longer vessels. Normal cardiac and venous valves are modeled as diodes, which permit flow of current in one direction only. Definitions of the symbols for circuit elements are provided in the legend. As indicated in Figure 1, current leaving the right side of the heart passes through the pulmonary system, first through the pulmonary artery capacitance, then the pulmonary capillary resistance, and then the pulmonary venous and left atrial capacitance, before entering the left ventricle. Current leaving the left side of the heart through the aortic valve can return to the right atrium via one of four pathways representing the vascular beds of the head and neck, myocardium, abdomen, and lower extremities.

The coronary circulation is modeled as a simple resistive pathway between the thoracic aorta and the right atrium. Separate, pulsatile voltage sources, modeled by components labeled VIN, can be applied between any of the vascular capacitors and ground potential, which represents zero (ambient atmospheric) pressure, to mimic external compression of these structures during CPR. In the present study, values for VIN were the same for all intrathoracic structures (i.e., a "thoracic pump" model of CPR was used).

Similar electrical models of the circulation have been described originally by Guyton [24] and by others [25-28]. In the present study we used the electrical circuit analysis program SPICE (Simulation Program for Integrated Circuit Evaluation) [29] to obtain solutions for instantaneous voltages at, and currents through, various test points or "nodes" in the circuit model on digital computer workstations. Minor changes were made in the previously published model [21, 22], for compatibility with the digital modeling approach, which is now used extensively by electrical engineers. In particular, to meet the technical requirements of SPICE software, a direct current (DC) path of some finite resistance is needed that connects the model to ground potential (i.e., a ground reference). If a low-resistance DC path were included, the result would be similar to a vascular puncture wound, allowing charge (blood) to leak from the circulatory system to the outside world. Accordingly, a very-high-resistance path (RGND, Fig. 1) was chosen, which allowed a negligible leak during the duration of the simulations. (A representative SPICE program for the circulatory model is available from the authors on request.)
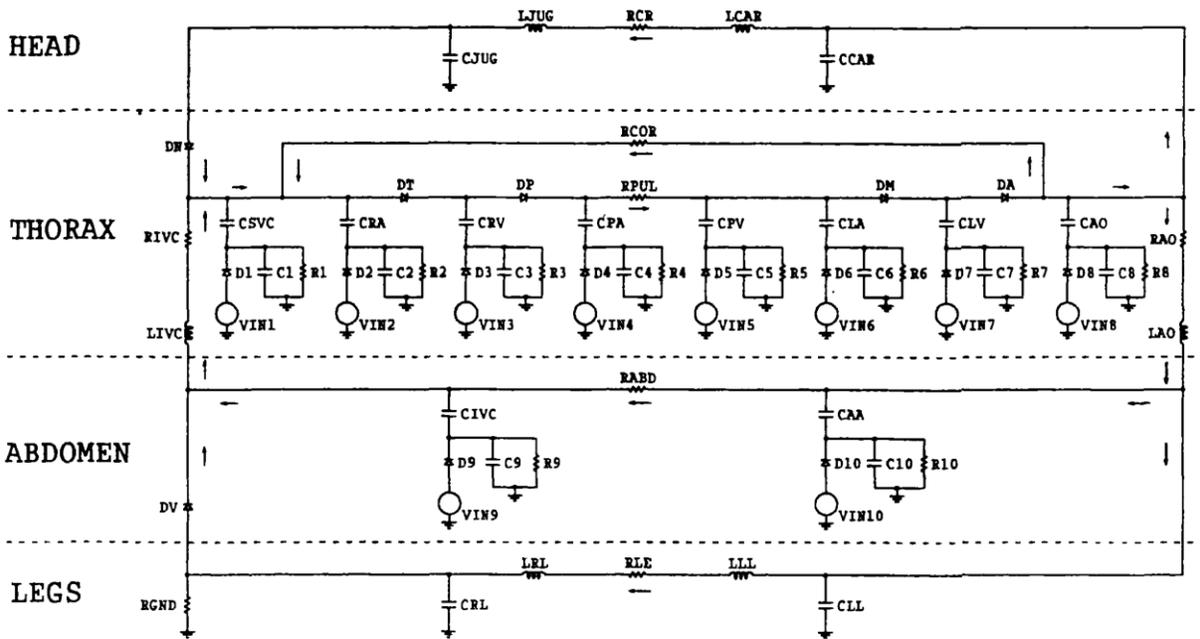
Figure 1. Circuit diagram of the model. Elements corresponding to vessels in the head, thorax, abdomen, and legs are identified. Capacitors (-||-) model large-vessel compliance; inductors (-ooooo-) model inertia; resistors (-∧∧∧∧-) model capillary beds; diodes (--|>|--) model valves. Voltage sources (--O--) are applied between earth ground and the thoracic and abdominal capacitors to model chest and abdominal compression. Arrows indicate direction of current flow. First letters identifying model components are C for capacitances, R for resistances, L for inductances, D for diodes (valves), and VIN for input voltage sources. The remaining letters of component labels indicate anatomic counterparts as follows: AA = abdominal aorta; A = aortic valve; ABD = abdominal capillaries; AO = thoracic aorta; CAR = carotid arteries; CR = cranial capillaries; COR = coronary capillaries; GND = ground; IVC = inferior vena cava; JUG = jugular veins; LA = left atrium; LE = legs; LL = lower limb arterial side; LV = left ventricle; M = mitral valve; N = Niemann's valve at the thoracic inlet; P = pulmonic valve; PA = pulmonary artery; PUL = pulmonary capillaries; PV = pulmonary veins; RA = right atrium; RL = lower limb right (venous) side; RV = right ventricle; SVC = superior vena cava; T = tricuspid valve; V = venous valves in legs. Parallel source resistances R1 through R10 (100 ohms) and capacitances C1 through C10 (0.1 microfarads) provided for a 0.1 sec rise time constant in real time and ensured release of external pressure during the relaxation phase.

Circuit Components

The initial values for the circuit components used in the model were the same as described previously [22]. Scale factors relating electrical to physiologic variables were 0.5 V = 1 mm Hg blood pressure (BP), 0.5 mA = 1 L/min blood flow, and 0.1 msec in simulation time = 1 sec in real-world time. Derivative scale factors for resistance and inertance were 1 mm Hg/(L/min) = 1,000 Ω, and 1 g/cm^4 = 1.259 mH. Typical values of resistance and capacitance of vascular beds were selected with reference to published literature [22] and scaled to represent a hypothetical 70-kg man with a normal, resting cardiac output (CO) of 5 L/min, arterial BP 120/80 mm Hg, and pulmonary artery pressure of 25/10 mm Hg. The effects of peripheral vasoconstriction caused by epinephrine were studied by increasing the normal peripheral vascular resistances of the abdomen and legs (RABD and RLE, Fig. 1) each by a factor of 5, in keeping with prior studies in animals [30=31].

External CPR

We modeled compression of the chest and abdomen by application of slightly damped rectangular voltage pulses from the sources shown in Figure 1. To approximate the damping factors of a real mechanical system, external compression pulses were constructed with an RC (resistive-capacitive) rise time constant of 0.1 sec in real-world time (10 psec in simulation time), provided by the filters R1, C1 through R10, C10 placed in parallel with each voltage source. Sources VIN1 through VIN10 were set to deliver rectangular pulses of durations lasting from 10% to 90% of total cycle time, as needed.

The thoracic sources, VIN1 through VIN8, were set to deliver current during the chest compression phase, and the abdominal sources, VIN9 and VIN10, were set to deliver current during the abdominal compression phase. Chest compression was modeled with a 80-mm Hg (40-V) pulse, representing the pressure transmitted through the chest wall to the surfaces of the heart and great vessels. This chest compression of 80 mm Hg represents peak internal thoracic pressure generated as a result of external chest compression. The 80-mm Hg value was selected as being realistic on the basis of prior animal studies [32] and in keeping with prior simulation studies using the electronic model [21]. All cardiac chambers and intrathoracic great vessels were compressed equally in these simulations according to the thoracic pump paradigm.

The abdominal compressions in simulations of IACCPR were added after a time delay equal to the length of the chest compression. Abdominal compression was modeled with a 100-mm Hg (50-V) pulse, representing the pressure transmitted through the abdominal wall to the surfaces of both the abdominal aorta and the inferior vena cava. To explore the effects of duty cycle on hemodynamics during standard and IAC-CPR, non-overlapping combinations of chest and abdominal compression times (10%/ 90%, 20%/80%, 30%/70%, etc.) were simulated at compression frequencies including 60 cycles/ min, 80 cycles/min, and 100 cycles/min.

Sampling Protocols

Simulated chest and abdominal compressions were begun with a stagnant circulation at time zero and continued until a steady state was reached. Generally, steady state was reached sooner for intermediate duty cycles near 50%/50% (chest/abdomen) than it was for the extreme cases of 10%/90% and 90%/10%. A digital sampling density of 100 samples/cycle was used to encompass all maximum and minimum values and to ensure accurate mean results. Digital values of the most informative data, based on results of preliminary studies--namely, aortic pressure, pulmonary flow, coronary flow, and cranial flow--were captured for ten complete compression cycles at steady state. Mean values for pressure and flow at steady state were found by averaging the 1,000 points in the time domain, spanning ten complete cycles. The non-pulsatile cases of 0% and 100% duty cycles were modeled using DC sources in SPICE. Plots were made using Matlab (The Math-Works, Inc., Natick, MA) or similar software.

RESULTS

Steady-state Sampling Intervals

Initial data were plotted vs. time to determine the time at which steady-state hemodynamics were established for each compression combination. For the extreme cases of 100%/0% and 0%/100% cycles, DC outputs were used. The transient responses to 90%/10% and 10%/90% were found to reach steady state at 100 real-time sec, so mean flows were taken for the range from 100 to 110 sec. For the 80%/20% and 20%/80% cases, steady state was reached at 50 real-time sec, and mean flows were computed from 50 to 60 sec. All other cases were evaluated from 30 to 40 sec after onset of CPR to meet the steady-state criterion. As a check of the steady-state criterion, mean pulmonary flow was compared with the sum of mean systemic flows in the cranial, coronary, abdominal, and lower extremity vascular beds, and agreement within 1% was obtained.

Waveforms

Figure 2 illustrates representative time domain waveforms for simulated aortic pressure, pulmonary flow, coronary flow, and cranial flow across one complete cycle of 50%/50% IAC-CPR at steady state. In these graphs, the full horizontal scale represents one compression cycle at a compression frequency of 80/min. The left half of each tracing represents the chest compression phase, and the right half of each tracing represents the abdominal compression phase. Cranial flow occurs primarily during chest compression, whereas coronary flow occurs primarily during abdominal compression. The waveforms for pressures and flows at compression frequencies of 60/min and 100/min were very similar to those shown in Figure 2.

Mean Aortic Pressure

Pulmonary Flow

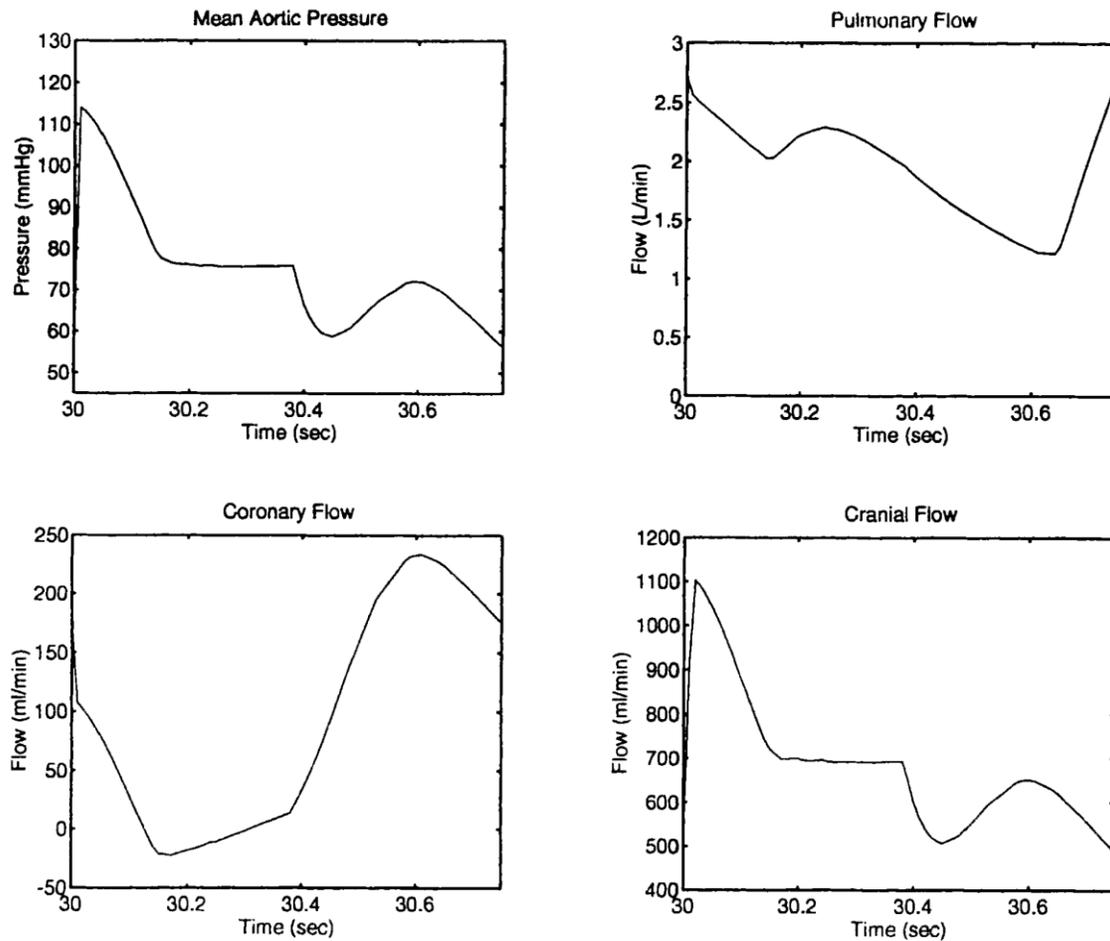**Coronary Flow**

Cranial Flow

FIGURE 2. Simulated time domain tracings of aortic pressure, pulmonary artery (total) flow, coronary flow, and cranial flow for one steady-state compression cycle of 50%/50% interposed abdominal compression CPR. The horizontal time base represents one compression cycle at 80 compressions/min, from 30 to 30.75 sec after onset of CPR. The first, left-hand half of the cycle represents the chest compression phase, and the second, right-hand half of the cycle represents the abdominal compression phase.

Duty Cycle Effects

The plots in Figure 3 illustrate thoracic aortic pressure, pulmonary flow, coronary flow, and cranial flow, as a function of the duty cycle during chest compression only (i.e., control CPR without IAC). Data are plotted for three different compression frequencies, 60/min (solid curves), 80/min (dashed curves), and 100/min (dotted curves). The outputs of the thoracic pump during CPR are relatively independent of compression frequency in the practical range from 60 to 100 compression cycles/ min, as has been previously described during conventional or standard CPR without abdominal compression, total (pulmonary) flow and coronary flow are maximized at 30% duty cycle for chest compression only. Cranial flow, however, increases steadily as a function of duty cycle in the range of 10% to 80%, as reported for earlier experimental studies of chest compression duration that measured ultrasonic Doppler flow velocity index in the carotid arteries [36].
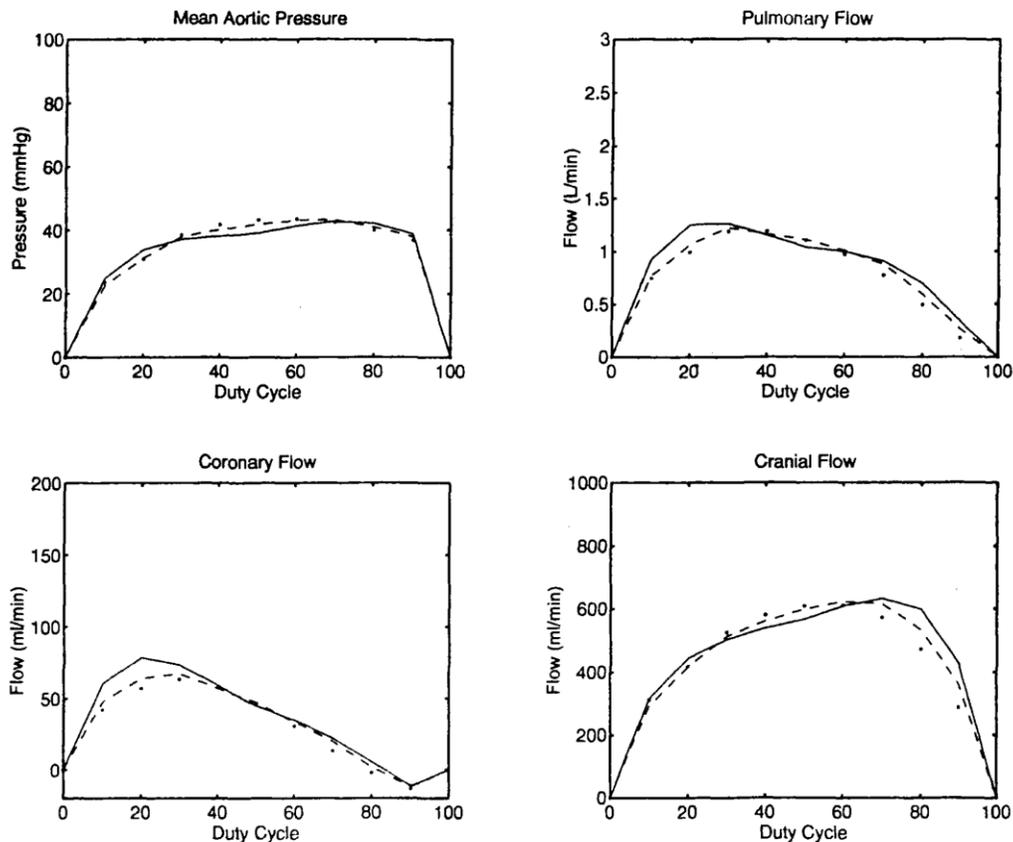

FIGURE 3. Mean aortic pressure, pulmonary artery (total) flow, coronary flow, and cranial flow for a computer-simulated human circulatory system during standard CPR at duty cycles for chest compression ranging from 0% to 100% percent of cycle time. Solid curves = 60 compressions/ min; dashed curves = 80 compressions/min; dotted curves = 100 compressions/min.

As shown in Figure 4 for 80-cycle/min CPR, the addition of IAC (solid curves) at 100 mm Hg, combined with thoracic pump CPR, improves total flow, myocardial flow, and cranial flow, compared with thoracic compression alone (dashed curves) at all duty cycle combinations. The results for 60 cycles/min and 100 cycles/min CPR were very similar to those for 80-cycles/min CPR. In terms of aortic pressure, total pulmonary flow, and coronary flow, the maximum average values during IAC-CPR occur at 30% chest compression time and 70% abdominal compression time. For cranial flow, the maximum occurs at 70%/30% chest/abdomen duty cycles; however, with IAC-CPR, cranial flow tends to plateau between 30% and 70% chest compression, so there is relatively little difference in cranial flow between the 30%/70% and 70%/30% techniques. Thus, overall, the optimal duty cycle for standard CPR is 30% chest compression time, 70% chest relaxation time; and the optimal duty cycle combination for IAC-CPR is 30% chest compression time, 70% abdominal compression time.
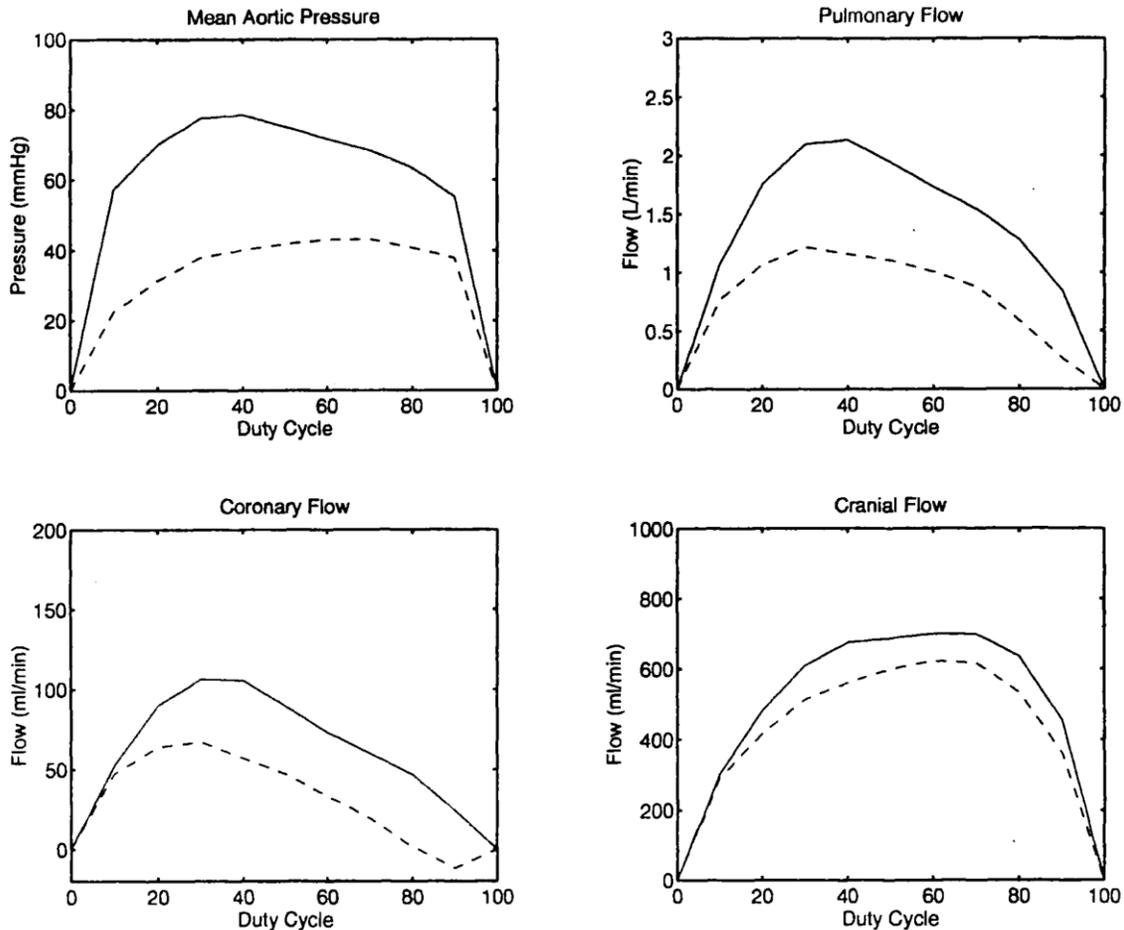

FIGURE 4. Mean aortic pressure, pulmonary artery (total) flow, coronary flow, and cranial flow for a computer-simulated human circulatory system during standard CPR (dashed curves) vs. interposed abdominal compression (1AC)-CPR (solid curves) at duty cycles for chest compression ranging from 0% to 100% percent of cycle time.

Peripheral Vasoconstriction

The plots in Figure 5 illustrate the effects of peripheral vasoconstriction, as would be produced by epinephrine. This effect was achieved by increasing the resistances of the legs and abdomen by a factor of five. The solid lines in Figure 5 represent complementary chest and abdominal compressions, and the dashed lines represent chest compression alone. The vertical scales are the same as in Figure 4. Peripheral vasoconstriction improves coronary and cranial flow, but total flow is decreased, as was found previously in animals [30]. Optimal compression cycle partitioning at 30%/70% chest/abdomen is not altered by peripheral vasoconstriction.
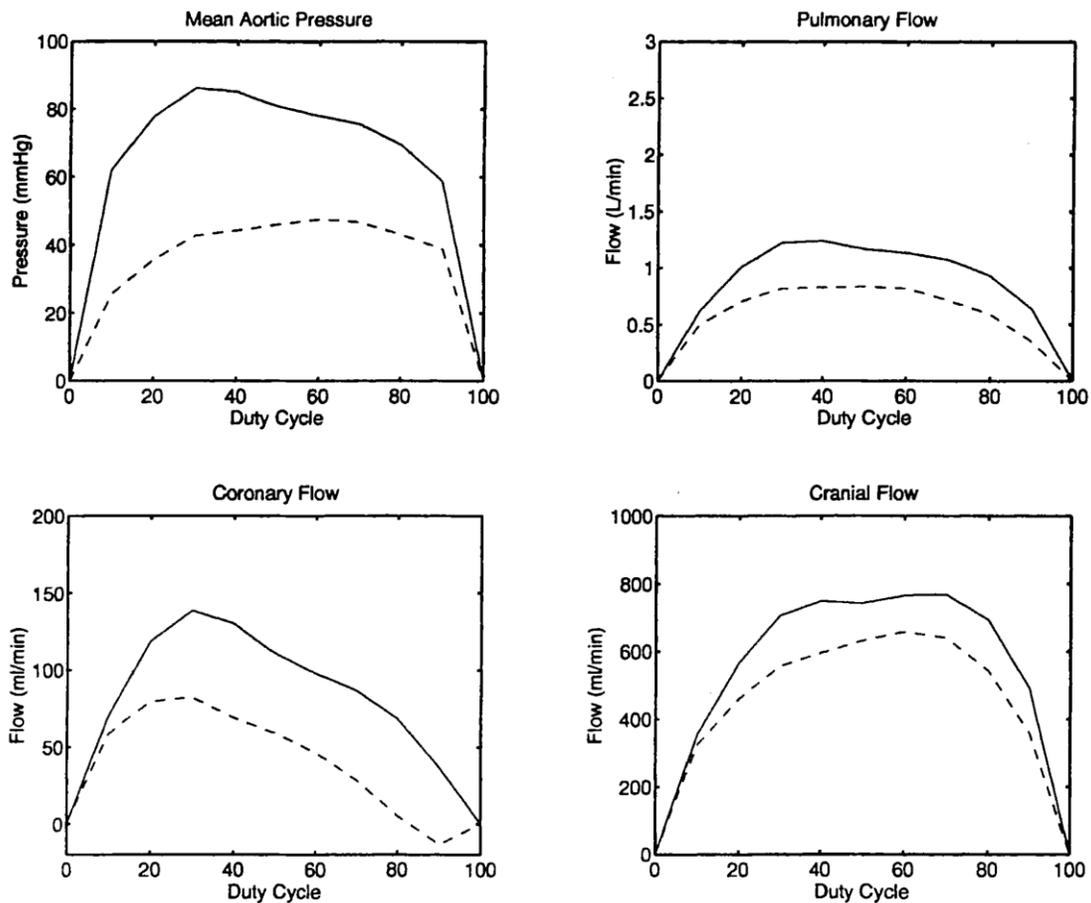

FIGURE 5. Mean aortic pressure, pulmonary artery (total) flow, coronary flow, and cranial flow for a computer-simulated human circulatory system in the presence of peripheral vasoconstriction simulating epinephrine effect. Standard CPR is indicated by dashed curves; interposed abdominal compression (IAC)-CPR is indicated by solid curves. During IAC-CPR, abdominal compression was always complementary to chest compression; e.g. when chest compression lasted 40% of cycle time, abdominal compression lasted 60% of cycle time. Chest compression frequency was 80/min. With peripheral vasoconstriction, total flow is reduced but vital organ perfusion is increased.

DISCUSSION

By modeling a complex biological system appropriately, an investigator can explore the implications of certain fundamental assumptions about how the system operates. In the present study we assumed that external pressures can impel blood (having inertial mass) to flow through resistive-capacitive networks forming a closed circuit similar to the mammalian circulatory system. The exploration of timing variables for conventional CPR and IAC-CPR in such a system suggests that the two innovative and nonstandard CPR modalities that have been shown to be effective both in animal studies and in clinical trials, namely IAC-CPR and HIC-CPR, can be profitably combined. Performance of IAC-CPR with HIC (i.e., shifting from 50% to 30% chest compression) is a clearly effective technique for enhancing systemic perfusion in the present model of the human circulatory system. The model predicts that the combined techniques can generate mean arterial pressures in excess of 75 mm Hg and artificial cardiac outputs in excess of 2.0 L/min, about 40% of normal resting cardiac output in man. These values begin to approach truly life-sustaining levels.

Manually performed chest compressions lasting approximately 30% of the compression cycle time can be practically generated according to a repeated three-count cadence: one-two-three, one-two-three, one-two-three, etc. Chest pressure is applied on the count of one and released on the count of two. For IAC-CPR, abdominal pressure is applied on the count of two, continued on the count of three, and released on the count of one. It is helpful to begin this rhythm with abdominal pressure on and chest pressure off; then switch pressure states on the counts of one and two.

Thus, in practice, the rescuer at the chest presses down on the count of one, releases pressure on the count of two, and is idle on the count of three. The rescuer at the abdomen releases pressure on the count of one, applies pressure on the count of two, and continues pressure on the count of three. (The reader may personally judge the simplicity of this cadence by performing simulated chest compression with the left hand and simulated abdominal compression with the right hand in pantomime.)

Graphic validation of the 30%/70% duty cycle produced by this method can be confirmed experimentally as follows. Fill the bladders of two ordinary clinical BP cuffs with air. Let one represent the "chest" and the other represent the "abdomen." Connect the air-loaded BP cuffs to pressure transducers and a two-channel graphic recorder. Then perform chest and abdominal compression on the two cuffs according to the one-two-three cadence just described. The degree to which a 30%/70% duty cycle is approximated by trainees after varying amounts of practice can be readily seen.

An important prediction of the present computer simulations is that coronary flow is particularly benefited by the combination of 30% chest compression and 70% abdominal counterpulsation. The importance of coronary perfusion pressure (CPP) in promoting return of spontaneous circulation (ROSC) after CPR has long been recognized [37-39]. Previous work by Ralston and coworkers in our laboratory [40] indicates that ROSC after 20 min of experimental CPR is almost certain when myocardial perfusion is > 25 mL/min/100 g and almost impossible when

myocardial perfusion is < 15 mL/min/100 g. One might therefore conceive of a "survival threshold" for myocardial perfusion near 20 mL/min/100 g that must be exceeded if the heart is to withstand prolonged resuscitation efforts. Under these circumstances the optimization of myocardial flow generated during external CPR may be lifesaving. If one assumes the weight of a human heart to be 300 to 400 g, coronary perfusion < 60 to 80 mL/min may be inadequate for ROSC in prolonged cardiac arrest and CPR. Reference to Figures 4 and 5 indicates that coronary flow for simulated standard CPR without IAC at 50% duty cycle lies very near the survival threshold. However, if either 30% chest compressions, IACs, or both are adopted, then simulated coronary flow can be promoted to levels above Ralston's proposed survival threshold. The simulations also suggest a rational mechanistic explanation for the observed effects on coronary perfusion. Because coronary perfusion occurs predominantly during chest recoil; a relatively longer perfusion time during "chest diastole" seems to favor mean coronary flow, as does the augmentation of diastolic CPP induced by IAC. Accordingly, the combined HIC-IAC modifications of present standard CPR may be especially important in promoting ROSC [39].

LIMITATIONS AND FUTURE QUESTIONS

The present study was conducted in a relatively simple electronic model of the circulation, including only 32 passive components and two peak pressure levels (chest and abdominal). Much more complex models have been described [27]. Our intent, however, was to capture the essence of the circulatory hernodynamics in cardiac arrest and CPR rather than to include all details, which are better studied in animal and in clinical models. For example, autoregulatory effects and effects of hypoxia causing minute-to-minute changes in peripheral vascular resistances of various organs were not modeled. Ventilatory pauses were not modeled, and complex schemes for coordinating ventilations and compressions to good effect were not explored. There may be possible benefits to such schemes; however, they must ultimately be simple enough to be executed in the chaotic setting of a cardiac arrest.

Mechanical factors acting on extravascular structures, such as diaphragmatic stabilization by IAC (during brief periods when rising abdominal compression may overlap falling chest compression) cannot be well studied by electronic models such as that described. In the present studies all vessels in the abdominal compartment were considered to be compressed equally, although suggestions as to improved IAC techniques [17] suggest that selective compression of the abdominal aorta is possible and may be of hemodynamic benefit. These limitations notwithstanding, we suggest that the differences in aortic pressures and regional blood flows as a function of the duty cycles for chest and abdominal compression, which are the main focus of the present study, are likely to persist in more complex models. Animal and eventually clinical studies will be required to verify these findings. It will be important to determine the feasibility of the three-count cadence technique described, including its effectiveness, and its safety.

With regard to safety, experimental studies have demonstrated that with high-impulse techniques, there is the potential for rib fracture even in healthy young experimental animals with flexible rib cages [3]. Such risk is probably greater in older humans with more brittle anterior chest walls. Nevertheless, 30%-duty-cycle CPR is highly likely to be safe in view of previous clinical experience at Duke University Hospital, where HIC-CPR has been practiced

extensively for more than two years without obvious ill effects [2]. The complications attributable to IAC in all clinical series have been few [5, 14, 41, 42]. Currently there is only one reported case of IAC-related abdominal organ damage among more than 300 resuscitated patients described in the literature [43]. Initial concerns regarding the possibility of more frequent emesis during IAC-CPR than during conventional CPR have remained unsubstantiated. Interestingly, in anesthetized dogs, IAC-CPR produces less gastric insufflation than does standard CPR when ventilation pressure is applied to both the trachea and the esophagus [44]. Hence, there is little evidence to suggest that either HIC-CPR alone or IAC-CPR alone cause more complications than does conventional, standard CPR. However, prospective trials combining these techniques should address both safety and efficacy.

CONCLUSION

Modeling of fluid flow through resistive capacitive networks mimicking human circulation identifies perfusion maxima for the combination of 30% chest compression with 70% abdominal compression times. A simple three-count rhythm can be established to approximate this theoretically optimal timing of external compressions during CPR using a manual technique. We conclude that combining 30%/70% chest and abdominal compressions is worthy of exploration in future experimental and clinical studies of external CPR.

REFERENCES

1. Maier GW, Tyson GS. Olsen CO, et al. The physiology of external cardiac massage: high-impulse cardiopulmonary resuscitation. Circulation. 1984; 70;86-101.

2. Maier GW. Newton JR. Wolfe JA, et al. The influence of manual chest compression rate on hemodynamic support during cardiac arrest: high-impulse cardiopulmonary resuscitation. Circulation. 1986; Suppl 1V):IV-51 - IV-59.

3. Swart GL, Mateer JR, DeBehnke DJ. Jameson, SJ, Osborn JL. The effect of compression duration on hemodynamics during mechanical high-impulse CPR. Acad Emerg Med. 1994; 1:430-7.

4. Swenson RD, Weaver WD, Niskanen RA, Martin J, Dahlberg S. Hemodynamics in humans during conventional and experimental methods of cardiopulmonary resuscitation. Circulation. 1988; 78:630-9.

5. Sack JB, Kesselbrenner MB. Hemodynamics, survival benefits, and complications of interposed abdominal compression during cardiopulmonary resuscitation. Acad Emerg Med. 1994; 1:490-7.

6. Babbs CF. Preclinical studies of abdominal counterpulsation in CPR. Ann Emerg Med..1984; 13(part 2):761-3.

7. Babbs CF, Tacker WA. Cardiopulmonary resuscitation with interposed abdominal compression. Circulation. 1986; 74(suppl IV): 37-41.

8. Babbs CF. Interposed abdominal compression-CPR: low technology for the clinical armamentarium. Circulation. 1992; 86:2011-12.

9. Ralston SH. Babbs CF. Niebauer MJ. Cardiopulmonary resuscitation with interposed abdominal compression in dogs. Anesth Analg. 1982; 61:645-51.

10. Voorhees WD. Niebauer MJ, Babbs CF. Improved oxygen delivery during cardiopulmonary resuscitation with interposed abdominal compressions. Ann Emerg Med. 1983; 12:128-35.

11. Berryman CR, Phillips GM. Interposed abdominal compression-CPR in human subjects. Ann Emerg Med. 1984; 13:226-9.

12. Howard M, Carrubba C. Foss F. et al. Interposed abdominal compression-CPR: its effects on parameters of coronary perfusion in human subjects. Ann Emerg Med. 1987; 16:253-9.

13. Ward KR, Sullivan RI, Zelenak RR, Summer WR. A comparison of interposed abdominal compression CPR and standard CPR by monitoring end-tidal PCO_2. Ann Emerg Med. 1989;18~831-7.

14. Sack JB, Kesselbrenner MB, Bregman D. Survival from in-hospital cardiac arrest with interposed abdominal counterpulsation during cardiopulmonary resuscitation. JAMA. 1992; 267:379-85.

15. Babbs CF. The evolution of abdominal compression in cardiopulmonary resuscitation. Acad Emerg Med. 1994; 1:469-77.

16. Ward KR. Possible reasons for the variability of human responses to IAC-CPR. Acad Emerg Med. 1994; 1:482-9.

17. Babbs CF. IAC-CPR: are we missing the mark in clinical trials? Am Heart J. 1993; 126:1035-41.

18. Adams CP. Martin GB, Rivers EP. Ward KR. Srnithline HA, Rady MY. Hemdynamics of interposed abdominal compression during human cardiopulmonary resuscitation. Acad Emerg Med. 1994; 1:498-502.

19. Ohomoto T, Miura I, Konno S. A new method of external cardiac massage to improve diastolic augmentation and prolong survival time. Ann Thorac Surg. 1976; 21:284-90.

20. Christenson JM, Hamilton DR, Scott-Douglass NW, Tyberg JV, Powell DG. Abdominal compressions during CPR: hemodynamic effects of altering timing and force. J Emerg Med. 1992; 10~257-66.

21. Babbs CF, Ralston SH, Geddes LA. Theoretical advantages of abdominal counterpulsation in CPR as demonstrated in a simple electrical model of the circulation. Ann Emerg Med. 1984; 13:660- 71.

22. Babbs CF, Weaver JC, Ralston SH, Geddes LA. Cardiac, thoracic. and abdominal pump mechanisms in CPR: studies in an electrical model of the circulation. Am J Emerg Med. 1984; 2:299-308.

23. Voytik SL, Babbs CF, Badylak SF. Simple electrical model of the circulation to explore design parameters for a skeletal muscle ventricle. J Heart Transplant. 1990; 9:160-74.

24. Guyton AC. Circulatory Physiology: Cardiac output and Its Regulation (First Edition). Philadelphia: W. B. Saunders, 1963, pp 138-9.

25. Cant J. Operation and instruction manual for the Cardiovascular Analog Trainer. Millis, Ma: Harvard Apparatus Company, 1974.

26. DePater L, van den Berg J. An electrical analogue of the entire human circulatory system. Med Biol Eng Comput. 1964; 2:161-6.

27. Attinger EO. Anne A. Simulation of the cardiovascular system. Ann N Y Acad Sci. 1966; 128:810-29.

28. Beneken JEW, DeWit B. A physical approach to hemodynamic aspects of the human cardiovascular system. In: Reeve EB. Physical Laws of Circulatory Transport: Regulation and Exchange. Philadelphia: W. B. Saunders, 1967.

29. Rashid MH. SPICE for Power Electronics and Electric Power. Englewood Cliffs, NJ: Prentice Hall, 1993.

30. Holmes HR, Babbs CF, Voorhees WD. deGaravilla B. Influence of adrenergic drugs upon vital organ perfusion during CPR. Crit Care Med. 1980; 8:137-40.

31. Chan RC. Babbs CF. Vetter RJ, Lamar CH. Abnormal response of tumor vasculature to vasoactive drugs. J Nat Cancer Inst. 1984; 72:145-50.

32. Babbs CF, Voorhees WD, Fitzgerald KR, Holmes HR, Geddes LA. Relationship of artificial cardiac output to chest compression amplitude-evidence for an effective compression threshold. Ann Emerg Med. 1983; 12:527-32.

33. Babbs CF. New versus old theories of blood flow during cardiopulmonary resuscitation. Crit Care Med. 1980; 8:191-5.

34. Yin CP, Cohen JM. Tsitlik J. Zola B, Weisfeldt ML. Role of carotid artery resistance to collapse during high-intrathoracic pressure CPR. Am J Physiol. 1982; 243:H259-H267.

35. Fitzgerald KR. Babbs CF, Frissora HA, Davis RW, Silver DI. Cardiac output during cardiopulmonary resuscitation at various compression rates and durations. Am J Physiol. 1981; 241:H442-H448.

36. Taylor GJ, Tucker WM, Greene HL, Rudikoff MT. Weisfeldt ML. Medical Intelligence- importance of prolonged compression during cardiopulmonary resuscitation in man. N Engl J Med. 1977; 296:1515-17.

37. Redding JS, Pearson JW. Resuscitation from ventricular fibrillation. JAMA. 1968; 203:255- 260.

38. Redding JS. Abdominal compression in cardiopulmonary resuscitation. Anesth Analg. 1971; 50:668-75.

39. Kern KB. Ewy GA, Voorhees:WD, Babbs CF, Tacker WA. Myocardial perfusion pressure: a predictor of 24-hour survival during prolonged cardiac arrest in dogs. Resuscitation. 1988; 16:241-50.

40. Ralston SH. Voorhees WD. Babbs CF. Intrapulmonary epinephrine during cardiopulmonary resuscitation: improved regional blood flow and resuscitation in dogs. Ann Emerg Med. 1984; 13:79-86.

41. Mateer JR. Steuven HA, Thompson BM, Aprahamian C, Darin J. Pre-hospital IAC-CPR versus standard CPR: paramedic resuscitation of cardiac arrests. Am J Emerg Med. 1985; 3:143-6.

42. Sack JB, Kesselbrenner MB, Jarrad A. Interposed abdominal compression CPR and resuscitation outcome during asystole and electromechanical dissociation. Circulation. 1992; 86:1692-700.

43. Waldman PJ, Walters BL, Grunau CFV. Pancreatic injury associated with interposed abdominal compressions in pediatric cardiopulmonary resuscitation. Am J Emerg Med. 1984; 2:510-12.

44. Babbs CF, Schoenlein WE, Lowe MW. Gastric insufflation during IAC-CPR and standard CPR in a canine model. Am J Emerg Med. 1985; 3:99-103.